Control of Nanoparticle Growth in High Temperature Reactor: Application of Reduced Population Balance Model II

Oluranti Sadiku[*] and Andrei Kolesnikov

*Department of Chemical and Metallurgical Engineering, Faculty of Engineering and the Built Environment,
Tshwane University of Technology, Private Bag X680, Pretoria 0001, Republic of South Africa*

Aerosol processes are often model using the population balance equation (PBE). This article presents a study on the simulation of particle size distribution during nanoparticle growth with simultaneous chemical reaction, nucleation, condensation and coagulation. The method used to reduce the population balance model is the method of moments. Under the assumption of lognormal aerosol size distribution, the method of moments was employed to reduce the original model into a set of first-order ODE's (ordinary differential equations) that accurately reproduce important dynamics of aerosol process. The objective of this study is to investigate if we can use the reduced population balance model for the control of nanoparticle size distribution and to investigate the process model sensitivity to the influence of disturbance. And subsequently use the model to control particle size distribution. The numerical result shows there is a dependence of the average particle diameter on the wall temperatures and disturbance has great influence on process model. The process model was used as a basis to synthesize a feedback controller where manipulated variable is the wall temperature of the reactor and the control variable the aerosol size distribution at the outlet of the reactor.

Keywords: Population Balance Equation, Method of Moments, Particle Size Distribution, Disturbance and Average Particle Diameter.

1. INTRODUCTION

In recent years, along with advancement in materials synthesis, it has been possible to embed nanoparticles with control size in bulk materials Zabarjadi et al.[1] Nanoparticles always have novel properties that can be used for the development of new improved processing, making the control synthesis of nanoparticles vital to fields like chemistry, materials science and engineering, and the environmental sciences. Again, nanosized (i.e., smaller than tens of nanometres) particles often behave differently, both physically and chemically, than their larger counterparts. Thus, the synthesis of model materials for the fundamental mechanisms of nanoparticle transformations, nucleation and growth as well as the physical and chemical properties of nanoparticle are critical to understanding their behaviour in natural engineered systems. Nanoparticles are of great scientific interest as they are effectively a bridge between bulk materials and atomic or molecular structures. A bulk material should have constant physical properties regardless of its size, but at the nano-scale this is not often the case. Size-dependant properties are observed such as quantum confinement in semiconductor particles, surface Plasmon resonance in some metal particles and superparamagnetism in magnetic materials. The properties of materials change as their size approaches the nanoscale and as the percentage of atoms at the surface of a material becomes significant.

Aerosol processes is one of major interest for the generation of nanopowders of nano- and micro-sized particles with well-defined product properties depending on particle characteristics such as primary particle size, specific surface area and agglomerate structure. These processes have largely replaced other processes which involve multiple steps of wet chemistry, due to the direct gas phase reaction of precursor vapour and the ease of separation of the particulate products from the gas. Strongly coupled aerosol systems exist in a number of applications

---

*Author to whom correspondence should be addressed.

including such diverse areas as materials synthesis, drug inhalation, nuclear reactor safety, multiphase combustion processes, pollution formation, flue gas cleaning and heat exchanger fouling and slagging. Aerosol product such as TiO_2, B_4C, find widespread use as pigments, reinforcing agents, ceramic powders, optical fibres, carbon blacks and semiconductor materials. Numerous experimental studies have suggested that aerosol growth occurs in stages, beginning with the gas phase chemical reaction of the reactants to produce monomers or molecules of the condensable species, Panagiotis.[2] The monomers form unstable clusters, which grow further by monomer condensation. Beyond a critical cluster size, nucleation of stable aerosol particles occurs. These particles grow further by coagulations (condensation and surface reaction of some other growth mechanisms, Kalani and Panagiotis[3]). In aerosol processes, the growth or coagulation rate, which is affected additively by Brownian and turbulent shear forces influences strongly on particle size, size distribution and morphology. And therefore, it is of fundamental interest in the synthesis of nanoparticles by aerosol processes. Numerical simulation provides a means of understanding and ultimately controlling the various dynamics, transport, and mass and energy coupling processes in aerosol systems.

A high temperature reactor for producing spherical nanoparticles from vapor phase is a multi-composition system; varying appreciably in the flow and temperature fields. Nanoparticle synthesized in high temperature reactor often carries certain charges, which can be further utilized in the electrostatic manipulation, measurement and control of such particles. The nanoparticles produced at high temperature often undergo rapid coalescence, with complex rate laws Michael and Markus.[4] There is a need for detailed understanding of nanoparticle formation especially the material synthesis and combustion in high temperature processes.

The dynamic model of aerosol processes are typically obtained from the application of population, material and energy balances, and consist of partial integro-differential equation systems (where the independent variables are time, space and one or more internal particle coordinates, such as particle volume and shape). Nonlinearity usually arises from complex reaction, nucleation, condensation and coagulation rates and their nonlinear dependence on temperature. The complex nature of aerosol process models has motivated an extensive research activity on the development of numerical methods for the accurate computation of their solution. Numerical models can be viewed as mathematical frameworks that permit the interaction of complex physical processes to be simulated. The first step in developing a numerical aerosol model is to assemble expressions for the relevant physical processes, such as chemical reactions, nucleation, condensation, coagulation,

etc. The next step is to approximate the particle size distribution with a mathematical size distribution function. The following are examples of solution methods.

Sectional methods (SM) are widely used to solve population equations. In these methods, the size spectrum is divided into a set of size classes. In so doing, distinguishes between zero-order and higher-order methods. Higher-order methods use low order polynomials to represent the particles within each section and can be regarded as a simple form of finite elements methods and will be discussed in the next section. They can suffer from stability problems and artificial dispersion; whereas zero-order methods are more robust. Using sectional methods, computational domain is divided into rather small intervals in which the solution is approximated by step functions. For each interval, one obtained an ordinary differential equation which is coupled to neighbours depending on the discretization scheme used. Debra and Sonia[5] described a single moment sectional model to simulate the evolution of an aerosol distribution that contains more than one chemical component. The proposed method is based on dividing the particle domain into X sections with time variant sections boundaries. To alleviate the problem with numerical diffusion in the presence of the surface growth, Kumar and Ramkrishna,[6–8] introduced a pivot technique combined with a moving grid and also the method of characteristics. An additional method set of equation is solved to ensure that a chosen set of properties is conserved. Vanni[9] coupled a sectional model to a detailed gas phase mechanism to calculate the soot particle size distribution in a continuous stirred tank reactor (CSTR).

An alternative to sectional methods are the more sophisticated finite element methods. In the finite element approach, the solution of the population balance is expanded in series of polynomials. For the coefficients of this expansion, a set of equations has to be solved and this is obtained by inserting the expansion into the population balance equation. Various methods can be derived by different nodes, functions, and time stepping schemes. The mathematical discipline of functional analysis provides the theoretical framework with which errors can be estimated. This is of course a very attractive feature of finite element methods.

Another alternative to sectional methods for solving the population balance equation are Monte Carlo (MC) methods. They are easy to implement, can account for fluctuations, and can easily incorporate several internal coordinates. In the case of nanoparticle modelling, the number of particles is so large that the fluctuations in particle numbers can be neglected.

One of the applications of Monte Carlo methods is the stochastic Monte Carlo (MC) method which is based on the principle that the dynamic evolution of an extremely large population of particles, *Np(t)*, can be followed by tracking down the relevant particle events (i.e., growth,

aggregation, nucleation). Meimaroglou et al.[10] used this method.

James and Panagiotis,[11] proposed a finite-dimensional approximation and control of nonlinear parabolic partial differential equation (PDE) systems by combining Galerkin's method with the concept of approximate initial manifolds, known as non-linear Galerkin's method. Aleck and Costas[12] used orthogonal collection of finite element methods to solve a continuous form of general population balance equation (PBE). Hailian et al.[13] developed a predictive controller for parabolic convection–diffusion–reaction systems operating in convection-dominated regimes, using the combination of finite differences approximation of the diffusion term and the method of characteristics. Dan et al.,[14] designed a control algorithm on the basis of finite dimensional models to capture the dominant dynamics of particulate processes. The least squares method (LSM) is a well-established technique for solving a wide range of mathematical problems. The basic idea in the LSM is to minimize the integral of the square of the residual over the computational domain, in the case when the exact solutions are sufficiently smooth the convergence rate is exponential. Daora and Jakobosen,[15] applied the least square method to solve the population balance equation.

The method of moments (MOM) is computationally the most efficient approach to obtain a numerical approximation to the moments of population balance. For this reason, this method is often used when simulating problems where transport of particles in a flow with complex geometry is essential. In the area of nanoparticle modelling, two techniques have been used so far. One of the techniques is the quadrature method of moments (QMOM) which is a more recent technique. Dorao and Jakobson[16] derived (QMOM) in two ways, i.e., the standard quadrature method of moments which is a numerical closure for method of moments (MOM) and the method of moments in the method of weighted residuals (MOM-MWR).

The second technique is the method of moment with internal closure (MOMIC). Diemer and Ehrman[17] developed a design for the comparison of reconstructed distributions from moment with direct calculation via sectional method. The design was used to probe sensitivity of distribution reconstruction and problem solution to model size for both the MOMIC and QMOM approaches. Barret and Webb[18] compared some approximation methods for solving the aerosol dynamic equation. The methods compared are quadrature method of moments, the finite element method (FEM), Luguerre quadrature and Associated Laguerre quadrature. Suddah and Mark[19] also used quadrature method of moments to solve the problem of obtaining closure of the moment equations, for the coagulation, growth, diffusion and thermophoretic terms to be expressed in their original forms.

In the first instance MOMIC has been developed to describe the formation and oxidation of soot particles. In its early form, the method is based on univariate description of spherical soot particles in the free molecular regime. An alternative approach for obtaining the moments of the PSD is the quadrature method of moments (QMOM). In this method, the moments are calculated assuming the PSD can be represented as weighted multidimensional Dirac delta function. The weights and the nodes are then chosen to satisfy the transport equations for the moments of the PSD. The advantage of this approach is that due to the choice of delta functions, there exists no closure problem. Gerber and Mousavi[20] applied the quadrature method of moments to the polydispersed droplet spectrum in transonic steam flows with primary and secondary nucleation.

The method of moments (MOM) is computationally the most efficient approach to obtain a numerical approximation to the moments of population balance. For this reason, this method is often used when simulating problems where transport of particles in a flow with complex geometry is essential. The dominant dynamic behaviour of many aerosol processes can be accurately captured by a model that describes the evolution of the three leading moments of aerosol size distribution.[21] The aim of this work is to investigate the sensitivity of the process model to the influence of disturbances and to use the reduced population balance model for the control of nanoparticle size distribution. The measurement of particle size distribution is a distinguishing feature in production of nanoparticles because the particle size provides the critical link between the product quality indices and the operating variables.[2] Thus, the ability to effectively control the shape of the PSD is essential for regulating the end product quality of the process. Many applications require a close control of this distributed particle length scale in order to achieve the highest performance.

2. PROCESS DESCRIPTION

The premixed preheated reactants (titanium tetrachloride and oxygen gas) are injected into the reactor where following exothermic reaction takes place. The products of these reactions are titania monomers and chlorine gas.

$$TiCl_4(g) + O_2(g) \rightarrow TiO_2(s) + 2Cl_2(g) \qquad (1)$$
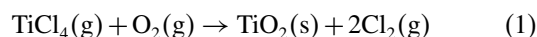
The size of a single TiO_2 molecule (monomer) is larger than the thermodynamic critical cluster size. As a result the difference between chemical reaction and nucleation cannot be noticed, thereby implying that the rapid chemical reaction leads to nucleation burst. The coagulation of TiO_2 monomers leads to an increase in the average particle size and a decrease in particle concentration.

2.1. Population Balance Model

The population balance equation consists of the following nonlinear partial integro-differential equation.[22]

$$\frac{\partial n}{\partial t} + \frac{\partial (G(v, z, \bar{x})n)}{\partial v} + c_z \frac{\partial n}{\partial z} - I(v^*)\delta(v - v^*)$$

$$= \frac{1}{2}\int_o^v \beta(\tilde{v}, v - \tilde{v}, \bar{x})n(\tilde{v}, z, t)n(v - \tilde{v}, z, t)\,d\tilde{v}$$

$$- n(v, z, t)\int_o^\infty \beta(v, \tilde{v})n(\tilde{v}, z, t)\,d\tilde{v} \qquad (2)$$

The first term on the left hand side of Eq. (2) describe the change in the number concentration of particle volume interval v, $v + dv$ and in the spatial interval z. $z + dz$, $n(v, z, t)$ denotes the particle size distribution function, v is particle volume, t is time, $z \in [0, L]$ is the spatial coordinate, L is the length of the process. The second term on the left hand side gives the loss or gain of particles by condensational growth, the third term on the left hand side which is $c_z(\partial n/\partial z)$ corresponds to the convective transport of aerosol particles at fluid velocity c_z and the fourth term on the left hand side accounts for the formation of new particles of critical volume v^* by nucleation rate I. $I(v^*)\delta(v - v^*)$, also accounts for gain and loss of particles by condensation. $G(v, z, \bar{x})$, $I(v^*)$ and $\beta(\tilde{v}, v - \tilde{v}, \tilde{x})$ are the nonlinear scalar functions and δ is the standard Dirac function. The mass and energy balance model which predicts the spatio-temporal evolution of the concentrations of species and temperature of the gas phase given by Ashish and Panagiotis[23] has the following form:

$$\frac{d\bar{x}}{dt} = \bar{A}\frac{d\bar{x}}{dz} + \bar{f}(\bar{x}) + \bar{g}(\bar{x})b(z)u(t)$$

$$+ \tilde{A}\int_0^\infty a(\eta, v, x)\,dv \qquad (3)$$

where $\bar{x}(z, t)$ is an n-dimensional vector of state variables that depends on space and time, $\bar{A}$, $\tilde{A}$ are constant matrices, $\bar{f}(\bar{x})$, $\bar{g}(\bar{x})$, $a(\eta, v, x)$ are nonlinear vector functions, $u(t)$ is the axially distributed manipulated input (e.g., wall temperatures, Tw_1 and Tw_2) and $b(z)$ is a known function which determines how control action $u(t)$, is distributed in space. The last term on the right hand side of Eq. (3) accounts for mass and heat transfer from the continuous phase to all the particles in population. The gain and loss of particles by Brownian coagulation is described by the first and second term on the right hand side of Eq. (2) respectively.

$$\frac{1}{2}\int_o^v \beta(\tilde{v}, v - \tilde{v}, \bar{x})n(\tilde{v}, z, t)n(v - \tilde{v}, z, t)\,d\tilde{v}$$

$$- n(v, z, t)\int_o^\infty \beta(v, \tilde{v})n(\tilde{v}, z, t)\,d\tilde{v} \qquad (4)$$

$G(v, z, \bar{x})$ and β are the condensational growth and collision frequency function, respectively for which two different expressions are used for free molecule size and continuum size regimes.[14] The free molecule size regime takes the following form:

$$G_{FM}(\bar{x}, v, z) = B_1 v^{1/3}(S - 1), \quad \text{where}$$

$$B_1 = (36\pi)^{1/3} v_1 n_s (k_B T / 2\pi m_1)^{1/2}$$

$$\beta_{FM}(\bar{x}, v, z) = B_2\left(\frac{1}{v} + \frac{1}{v}\right)^{1/2}(v^{1/3} + \bar{v}^{1/3})^2$$

$$B_2 = (3/4\pi)^{1/6}(6k_B T v_1 / m_1)^{1/2} \qquad (5)$$

And the continuum size regime takes the following form:

$$G_C(\bar{x}, v, z) = B_3 v^{1/3}(S - 1), \quad \text{where}$$

$$B_3 = (48\pi^2)^{1/3} D v_1 n_s, \quad D = \lambda(8k_B T / \pi m_1)^{1/2}/3$$

$$\beta_C = B_4\left(\frac{C(v)}{v^{1/3}} + \frac{C(\bar{v})}{\bar{v}^{1/3}}\right)(v^{1/3} + \bar{v}^{1/3}), \quad B_4 = \frac{2k_B T}{3\mu} \qquad (6)$$

In Eqs. (5) and (6), T is the temperature, S is the saturation ratio, D is the condensable vapour diffusivity, λ is the mean free path of the gas, μ is the fluid viscosity, n_s is the monomer concentration at saturation. ($n_s = P_s/k_B T$, where P_s is the saturation pressure), m_1 is the monomer mass, v_1 is the monomer volume, r is the particle radius, $C(v) = 1 + B_5\lambda/r$ is the Cunningham correction factor and $B_5 = 1.257$. Lastly, the nucleation rate $I(v^*)$ is assumed to follow the classical Becker-Doring theory given by the expression below (Pratisinis).[24]

$$I = n_s^2 s_1 (k_B T / 2\pi m_1)^{1/2} S^2 (2/9\pi)^{1/3}$$

$$\times \sum^{1/2} \exp(-k^* InS/2) \qquad (7)$$

where s_1 is the monomer surface area and k^* is the number of monomer in critical nucleus and is given by:

$$k^* = \frac{\pi}{6}\left(\frac{4\sum}{InS}\right)^3, \quad \text{where}$$

$$\sum = \gamma v_1^{2/3}/k_B T \text{ and } \gamma \text{ is the surface tension} \qquad (8)$$

3. LOGNORMAL AEROSOL SIZE DISTRIBUTION

The population balance model in Eq. (2) is highly complex and does not allow the direct use for numerical computation of the size distribution in real-time. To overcome this problem and to accelerate the computations, method of moments was employed to reduce the population balance model to a set of ODEs for the moments of the size distribution. In order to describe the spatio-temporal evolution of the three leading moments of the volume distribution (which describes the exact evolution of the lognormal aerosol size), a lognormal function was employed in moment model, which was applied to population balance model.

3.1. Moment Model

We assumed that the aerosol size distribution can be adequately represented by lognormal function which is described as:

$$n(v, z, t) = \frac{1}{3v} \frac{1}{\sqrt{2\pi} In\sigma} \exp\left[-\frac{In^2(v/v_g)}{18In^2\sigma}\right] \quad (9)$$

where v_g, is the geometric average particle volume and σ is the standard deviation. The kth moment of the distribution is defined as:

$$M_k(t) = \int_0^\infty v^k n(v, z, t)\, dv \quad (10)$$

According to the properties of a lognormal function, any moment can be written in terms of M_0, v_g, and σ as follows:

$$M_k = M_0 v_g^k \exp\left(\frac{9}{2} k^2 In^2 \sigma\right) \quad (11)$$

If Eq. (11) is written for $k = 0$, 1, and 2, then v_g and σ can exactly be expressed in terms of the first three moments of the distribution according to the following relations:

$$In^2\sigma = \frac{1}{9} In\left(\frac{M_0 M_2}{M_1^2}\right) \quad \text{and} \quad v_g = \frac{M_1^2}{M_0^{3/2} M_2^{1/2}} \quad (12)$$

In this subsection, the ODEs describing the temporal evolution of the three leading moments of the size distribution for the free molecule size and continuum size regime are presented.

3.1.1. Free Molecule Size Regime

The ODE system that describes the spatio-temporal size distribution of the kth moment of the aerosol size distribution is computed by substituting Eq. (5) into Eq. (2), multiplying by v^k, and integrating over all particle sizes. That gives the temporal evolution of the zeroth moment which is affected by nucleation and coagulation:

$$\frac{dM_0}{dt} = -c_z \frac{dM_o}{dz} + I - B_2 b_0 (M_0 M_{1/6} + 2M_{1/3} M_{-1/6} + M_{2/3} M_{-1/2}) \quad (13)$$

where the coefficient b_0 is used for the relationship:

$$\left(\frac{1}{v} + \frac{1}{\bar{v}}\right)^{1/2} = b_0\left(\frac{1}{v^{1/2}} + \frac{1}{\bar{v}^{1/2}}\right) \quad (14)$$

and it was computed by the expression $b_0 = 0.633 + 0.092\sigma^2 - 0.022\sigma^3$ in publication of Pratisinis.[24] The evolution of M_1 (aerosol volume), which is affected by condensation is given by

$$\frac{dM_1}{dt} = -c_z \frac{(dM_1)}{dz} + Iv^* + B_1(S-1)M_{2/3} \quad (15)$$

And the second moment, M_2, depends on nucleation and coagulation according to the formula:

$$\frac{dM_2}{dt} = -c_z \frac{dM_2}{dz} + Iv^{*2} + 2B_1(S-1)M_{5/3} + 2b_2 B_2(M_{7/6}M_1 + 2M_{4/3}M_{5/6} + M_{1/2}M_{5/3}) \quad (16)$$

where b_2 is used as b_0 but for coagulation kernel of the second moment b_2 is computed by the expression: $b_2 = 0.39 + 0.5\sigma - 0.214\sigma^2 + 0.029\sigma^3$ (Pratisinis).[24]

3.1.2. Continuum Size Regime

The spatio-temporal evolution of the kth moment of the aerosol size distribution in the continuum regime is computed by substituting Eq. (6) into Eq. (2), multiplying by v^k, and integrating over all particle sizes gives the temporal evolution of the zeroth moment M_0, M_1 and M_2

$$\frac{dM_0}{dt} = -c_z \frac{dM_0}{dz} + I - B_4\left[M_0^2 + M_{1/3}M_{-1/3} + B_5\lambda\left(\frac{4\pi}{3}\right)^{1/3} \cdot (M_0 M_{-1/3} + M_{1/3}M_{-2/3})\right] \quad (17)$$

$$\frac{dM_1}{dt} = -c_z \frac{dM_1}{dz} + Iv^* + B_3(S-1)M_{1/3} \quad (18)$$

$$\frac{dM_2}{dt} = -c_z \frac{dM_2}{dz} + Iv^{*2} + 2B_3(S-1)M_{4/3} + 2B_4\left[M_1^2 M_{4/3}M_{2/3} + B_5\lambda\left(\frac{4\pi}{3}\right)^{1/3} \cdot (M_1 M_{2/3} + M_{1/3}M_{4/3})\right] \quad (19)$$

4. ANALYSIS OF RESULTS AND DISCUSSION

This section describes the application of moment model of the aerosol flow reactor for the purpose of nonlinear control of the reactor. Under the assumption of lognormal aerosol size distribution, the mathematical model that describes the evolution of the first three moments of distribution, together with the monomer and reactant concentration and temperature takes the following form.

$$\frac{dN}{d\theta} = -c_{zl}\frac{dN}{d\bar{z}} + I' - \xi N^2$$

$$\frac{dV}{d\theta} = -c_{zl}\frac{dV}{d\bar{z}} + I'k^* + \eta(S-1)N$$

$$\frac{dV_2}{d\theta} = -c_{zl}\frac{dV_2}{d\bar{z}} + I'k^{*2} + 2\varepsilon(S-1)V + 2\zeta V^2$$

$$\frac{dS}{d\theta} = -c_{zl}\frac{dS}{d\bar{z}} + C\bar{C}_1\bar{C}_2 - I'k^* - \eta(S-1)N$$

12

J. Comput. Theor. Nanosci. 8, 8–16, 2011

$$\frac{d\bar{C}_1}{d\theta} = -c_{zl}\frac{d\bar{C}_1}{d\theta} - A_1\bar{C}_1\bar{C}_2$$

$$\frac{d\bar{C}_2}{d\theta} = -c_{zl}\frac{d\bar{C}_2}{d\theta} - A_2\bar{C}_1\bar{C}_2$$

$$\frac{d\bar{T}}{d\theta} = -v_{zl}\frac{d\bar{T}}{d\bar{z}} + B\bar{C}_1\bar{C}_2\bar{T} + E\bar{T}(\bar{T}_w - \bar{T}) \qquad (20)$$

$$\xi = \frac{\xi_{FM}\xi_C}{\xi_{FM} + \xi_C}$$

$$\xi_C = K\left[1 + \exp(In^2\sigma) + B_5(K_{n_1}/r_g')\right.$$

$$\left.\times \exp\left(\frac{1}{2}In^2\sigma\right)(1 + \exp(2In^2\sigma))\right]$$

$$\xi_{FM} = r_g'^{1/2}b_0\left[\exp\left(\frac{25}{8}In^2\sigma\right) + 2\exp\left(\frac{5}{8}In^2\sigma\right)\right.$$

$$\left. + \exp\left(\frac{1}{8}In^2\sigma\right)\right] \qquad (21)$$

$$\eta = \frac{\eta_{FM}\eta_C}{\eta_{FM} + \eta_C}, \qquad \eta_{FM} = v_g'^{2/3}\exp(2In^2\sigma) \quad \text{and}$$

$$\eta_C = \frac{4K_{n_1}}{3}v_g'^{1/3}\exp\left(\frac{1}{2}In^2\sigma\right) \qquad (22)$$

$$\varepsilon = \frac{\varepsilon_{FM}\varepsilon_C}{\varepsilon_{FM} + \varepsilon_C}, \qquad \varepsilon_C = \frac{4K_{n_1}}{3}v_g'^{1/3}\exp\left(\frac{7}{2}In^2\sigma\right) \quad \text{and}$$

$$\varepsilon_{FM} = v_g'^{2/3}\exp(8In^2\sigma) \qquad (23)$$

$$\zeta = \frac{\zeta_{FM}\zeta_C}{\zeta_{FM} + \zeta_C}$$

$$\zeta_{FM} = r_g'^{1/2}b_2\exp\left(\frac{3}{2}In^2\sigma\right)$$

$$\times\left[\exp\left(\frac{25}{8}In^2\sigma\right) + 2\exp\left(\frac{5}{8}In^2\sigma\right)\right.$$

$$\left. + \exp\left(\frac{1}{8}In^2\sigma\right)\right]$$

$$\zeta_C = K\left[1 + \exp(In^2\sigma) + B_5(K_{n_1}/r_g') \times \exp\left(-\frac{1}{2}In^2\sigma\right)\right.$$

$$\left.\times\left(1 + \exp(-2In^2\sigma)\right)\right] \qquad (24)$$

where $\bar{C}_1$ and $\bar{C}_2$ are the dimensionless concentrations of the reactants, $\bar{T}_w$, $\bar{T}$ are the dimensionless reactor and wall temperature, respectively, A_1, A_2, B, C, E are the dimensionless quantities. Table II gives the process parameters used in the simulation.

Dimensionless quantities for the model of Eq. (20), according to Ashish and Panagiotis[23]

$$A_1 = \tau k P_0 y_{20}/RT_0, \qquad A_2 = \tau k P_0 y_{10}/RT_0,$$

$$B = P_0 k\tau\Delta H_R y_{10}y_{20}/RT_0^2 C_P, \qquad \bar{C}_i = y_i/y_{10}\bar{T},$$

$$C = N_{av}k\tau y_{10}y_{20}(P_0/RT_0)^2/n_{s0}, \qquad E = 4URT_0\tau/DC_pP_0,$$

Table I. Dimensionless variables by Ashish and Panagioti.

$N = M_0/n_s$, $V = M_1/n_s v_1$	Aerosol concentration and volume
$V_2 = M_2/n_s v_1^2$	Second aerosol moment
$\tau = (2\pi m_1/k_B T)^{1/2}n_s s_1$	Characteristic time for particle growth
$K = (2k_B T/3\mu)n_s\tau,$	Coagulation coefficient and Nucleation rate
$\quad I' = I/(n_s/\tau)$	
$K_{n_1} = \lambda/r_1$	Knudsen number
$v_g' = v_g/v_1$	Dimensionless geometric volume
$r_g' = r_g/r_1$	Dimensionless geometric radius
$\bar{z} = z/L$	Dimensionless distance
$c_{zl} = \tau c_z/L,$ $\theta = t/\tau$	Dimensionless velocity and time
$\theta = t/\tau$	Dimensionless time

$$\bar{T} = T/T_0 \quad \text{and} \quad \bar{T}_w = T_w/T_0$$

In this chapter, the process model of the equations in Eq. (20) was numerically solved in by using simulink, a part of (Matlab) soft ware environment; it is an interactive computing package for simulating and analysing differential equations, mathematical models and dynamic systems. The computation was done using a multi step solver known as ode 15s (stiff/NDF) solver, ode 15s is a variable-order solver based on the numerical differentiation formulas (NDFs). Optionally it uses the backward differential formulas BDFs Sergey.[25] Table II shows the process variable parameters used for solving the process model of Eq. (20).

Since the objective of this study is to control nanoparticle growth with desired particle distribution in high temperature reactor, we studied the effect of wall temperature

Table II. Process model parameters for the simulation study.

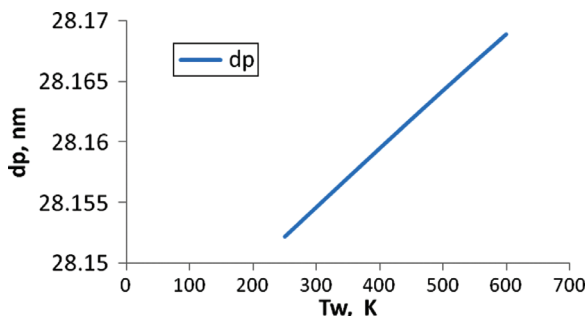|	
$L = 1.5$ m	Reactor length
$D = 0.01$ m	Reactor diameter
$P_0 = 101000$ pa	Process pressure
$T_0 = 2000$ K	Inlet temperature
$y_{10} = 0.4$	Inlet mole fractions of O_2
$y_{20} = 0.6$	Inlet mole fractions of $TiCl_4$
$U = 160$ J m^{-2} s^{-1} K^{-1}	Overall coefficient of heat transfer
$\Delta H_R = 88000$ J mol^{-1}	Heat of reaction
$C_P = 1615.25$ Jmol^{-1}K^{-1}	Heat capacity of process fluid
$MW_g = 14.0 \times 10^{-3}$ kg mol^{-1}	Mol wt. of process fluid
$K = 11.4$ m^3 mol^{-1}s^{-1}	Reaction rate constant
$\mu = 6.7 \times 10^{-5}$ kg m^{-1} s^{-1}	Viscosity of process fluid
$\log P_s(mmHg)$	PVT relation
$\quad = -4644/T + 0.906\log T$	
$\quad -0.00162T + 9.004$	
$\gamma = 0.08$ N m^{-1}	Surface tension
$v_1 = 5.33 \times 10^{-29}$ m^3	Monomer volume
$N_{av} = 6.023 \times 10^{23}$#mol^{-1}	Avogadro's constant
$R = 8.314$ J mol^{-1} K^{-1}	Universal gas constant
$k_B = 1.38 \times 10^{-23}$ JK^{-1}	Boltzmann's constant
$\sigma = 0.5$	Sigma
$r_g = 1.5e06$ μm	Geometric radius
$r_1 = 0.5e06$ μm	Monomer radius
$v_g = \pi dp^3/6$	Geometric volume
$s_0 = 1.1587E - 19$ m	Monomer surface area
$T_w = 800$ K, 500 K	Wall temperature
$Re = 2000$	Reynolds number

Fig. 1. Average particle diameter as function of the wall temperature.

bi-particle collision increases resulting in a sharp increase in particle diameter. Several simulation runs were performed to investigate the effect of disturbances of $TiCl_4$, O_2 flow rate on average particle diameter with respect to the model parameters. The disturbances actually affect the model because it made the system to be unstable. And because the process model is highly nonlinear, the influence of disturbance on average particle diameter is nonstationary (random walk). Figure 3 shows the effect of

on average particle diameter. It is a variable that could be used in industry to control the aerosol size distribution. The effect of wall temperature on average particle diameter was investigated in the open-loop simulation in order to use the model as a basis to synthesize feedback controllers which manipulated the input (wall temperatures) in order to achieve control of nanoparticle size and its distribution. From the Figure 1 it was found that the particle size increases with increasing wall temperature which clearly shows that the wall temperature is a variable that has significant effect on the average particle diameter.

It is important to point out that in our studies, we have calculated the dimensionless time for the process in order to observe the sensitivity of the disturbance on average particle diameter. (Table I shows the dimensionless variable). The residence time of particle distribution is intimately related to the average flow velocity and characteristics time of particle growth and they are useful because they are used in calculating the dimensionless time (θ). The dimensionless time (θ), t/τ is equal to 7e06. Figure 2, shows the average particle diameter as function of dimensionless time.

The dimensionless time affect the particle aerosol characteristics [average size]. The average particle diameter here increases with increase of the dimensionless time. One can see from this graph that when particles are nucleated, a primary particle with diameter of about 400 nm is produced at constant time. After a certain number of particles have been produced the frequency of
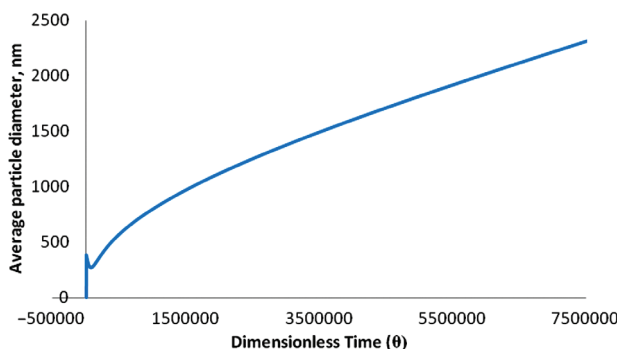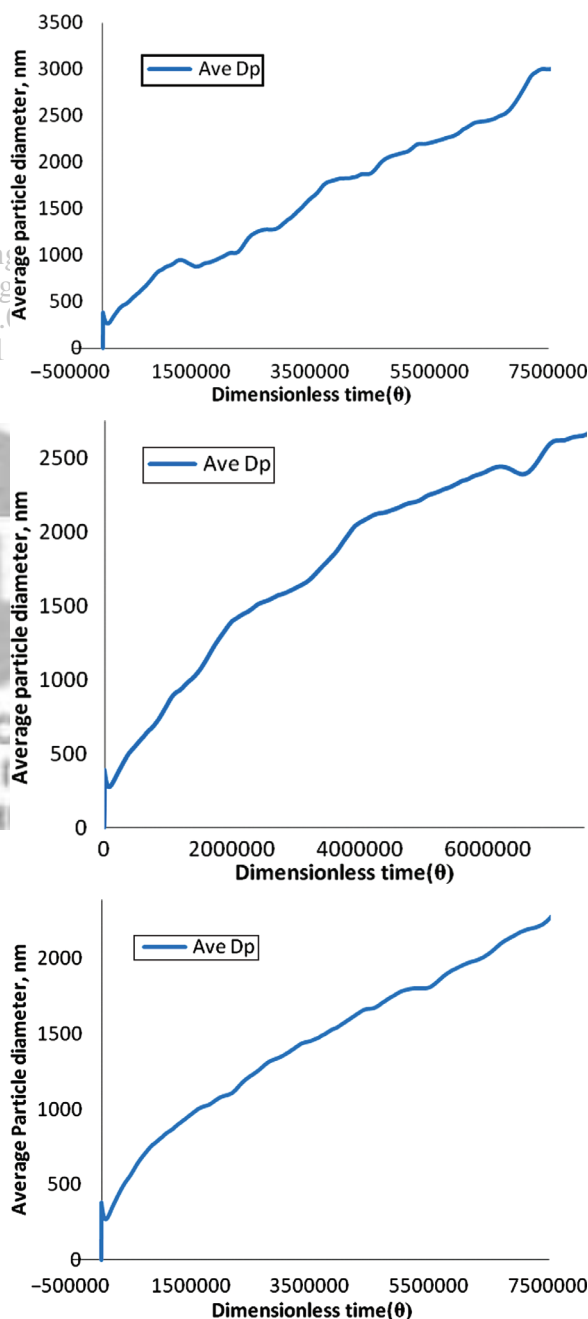
Fig. 2. Average particle diameter as function of dimensionless time.

Fig. 3. Top plot, effect of $TiCl_4$ and O_2 disturbances on average particle diameter. Middle plot, effect of O_2 disturbance on average particle diameter and bottom plot, effect of $TiCl_4$ on average particle diameter.
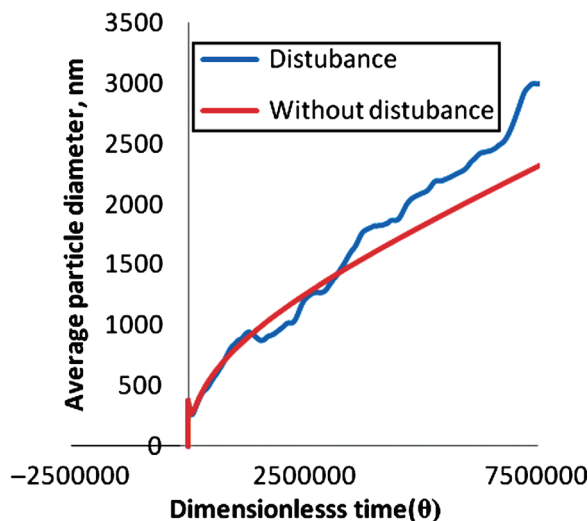
14

J. Comput. Theor. Nanosci. 8, 8–16, 2011

Fig. 4. Comparison of average particle diameter with and without disturbance.

disturbances of $TiCl_4$, O_2 flow rate on average particle diameter. For this dimensionless time one could observed that disturbances to have great effect on the outputs, thus the need to control particle size distribution.

Figure 4 shows the comparison of the average particle diameter with and without disturbances. It can be observed that the influence of disturbance resulted to unstable process. The result of average particle diameter without distubance shows the process is not distort while that of disturbance shows instability, this attributed to the fact that the disturbance distort the process.

4.1. Closed Loop Simulation

The control problem was formulated as one of tracking the average particle diameter of the aerosol system along a time-varying profile, by manipulating the wall temperature, i.e., $y(t) = dp(t)$ and $u(t) = Tw$. The effect of wall temperature on average particle diameter was investigated through the open loop simulation and was found that the process model could be used to control particle size distribution. Therefore the model of Eq. (20) was used as
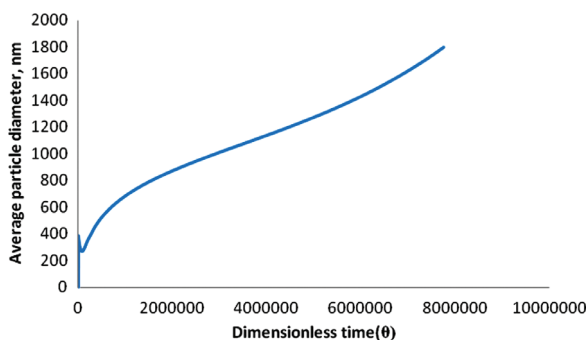

Fig. 5. Closed-loop profiles of average particle diameter in the outlet of the reactor with −0.23% error.
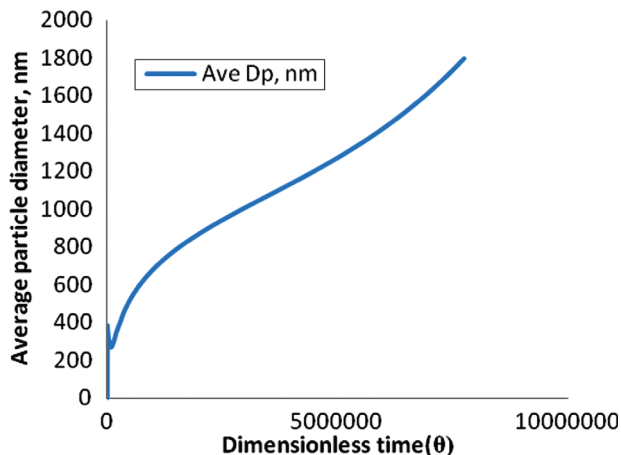

Fig. 6. Closed-loop profiles of average particle diameter in the outlet of the reactor with −0.03% error.

the basis for the synthesis of proportional–integral controller utilizing the control method with $k = 0.1$ and $\tau = 4 \times 10^{-10}$. (k and τ were computed after extensive trial and errors). The proposed controller regulate the particle diameter with minimum percentage error to its new set point value. Figures 5 and 6 shows the controlled output of average particle diameter (from $t = 0$ to 7.75e06) with −0.23% and 0.03% error respectively. The wall temperature is not manipulated directly but indirectly through manipulation of inlet flow rate and dimensionless temperature. To this end controller should be designed base on an ODE model that describes the dynamics that operates in an internal loop to manipulate the inlet flowrate and dimensionless temperature to ensure that the average particle diameter obtains the values computed by the controller.

The objective of closed loop simulation is to show that the use of feedback control allows producing an aerosol product with a desired average particle diameter ($dp = 1800$ nm). It is clear that the use of feedback control allows producing an aerosol product with particle diameter that exactly matches the desired one and sometimes almost matches the desired one with minimal error.
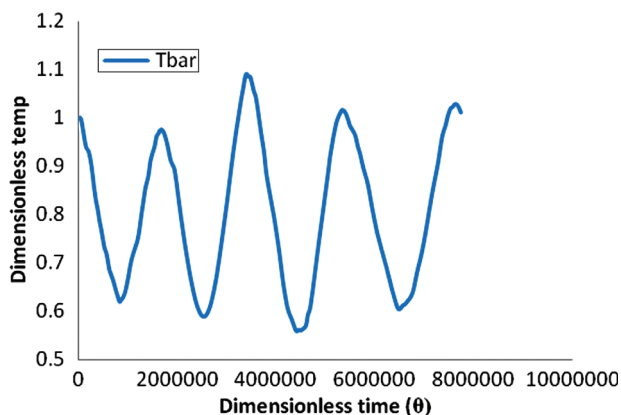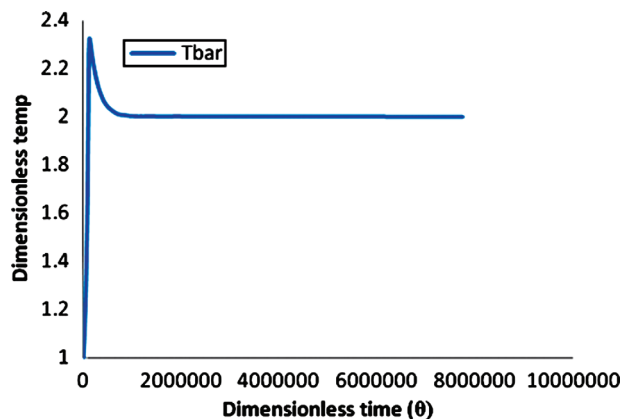

Fig. 7. Manipulated input profile.

Fig. 8. Manipulated input profile.

The manipulated input profile of Figures 7 and 8 are smooth functions of dimensionless time. It is important to note that the wall temperature was manipulated in the last equation of Eq. (20) which is the dimensionless temperature, thus the effect of the manipulated input profile is shown in the dimensionless temperature.

5. CONCLUSION

In this work, we used the application of the reduced population balance model for the control of nanoparticle size distribution. The model accounts for simultaneous nucleation, condensation and coagulation for the control of size distribution. Under the assumption of lognormal size distribution, the method of moment was employed to reduce the population balance model into the simpler model, describing the evolution of the first three leading moment. This simplified model is a set of ODEs. The effect of wall temperature on average particle diameter was investigated in order to synthesize nonlinear output feedback controllers for titanium aerosol reactor that attain size distributions with desired characteristics. The average particle diameter can be increased by increasing the reactor wall temperature. The performance of the open loop simulation was verified through computer simulation using another soft ware. Based on the sensitivity of wall temperature upon the particle diameter d_p, we investigated the

process model sensitivity to the influence of disturbance. The process model was subsequently used as a basis to synthesize a feedback controller which manipulates the wall temperature of the reactor to control the aerosol size distribution in the outlet of the reactor with desired average particle diameter.

References

1. M. Zabarjadi, K. Esfarjani, A. Shakori, Z. Bian, J. Bahk, Z. Gehong, J. Bowers, H. Lu, J. Zide, and A. Gossard, *J. Electron. Mater.* 38, 954 (**2009**).
2. D. C. Panagiotis, Model Based Control of Particulate Processes, Springer, New York (**2002**).
3. A. Kalani and D. C. Panagiotis, *Aerosol Sci. Technol.* 32, 369 (**2000**).
4. G. Michael and K. Markus, *Journal of Computational Physics* 183, 210 (**2002**).
5. Y. H. Debra and M. K. Sonia, *Journal of Atmospheric Environment* 32, 1701 (**1998**).
6. S. Kumar and D. Ramkrishna, *Chem. Eng. Sci.* 51, 1311 (**1996**).
7. S. Kumar and D. Ramkrishna, *Chem. Eng. Sci.* 51, 1333 (**1996**).
8. S. Kumar and D. Ramkrishna, *Chem. Eng. Sci.* 52, 4659 (**1997**).
9. M. Vanni, *J. Colloid Interface Sci.* 221, 143 (**2000**).
10. D. Meimaroglou, A. I. Roussos, and C. Kiparissides, *Chem. Eng. Sci.* 61, 5620 (**2006**).
11. B. James and D. C. Panagiotis, *International Journal of Control* 73, 439 (**2000**).
12. A. H. Aleck and A. K. Costas, *Journal of Chemical Engineering Science* 60, 4157 (**2005**).
13. S. Hailian, J. F. Fraser, and G. Martin, *Journal of Process Control* 17, 379 (**2007**).
14. S. Dan, H. E. F. Nael, L. Mingheng, M. Prashant, and D. C. Panagiotis, *Chem. Engng. J.* 6, 268 (**2006**).
15. C. A. Dorao and H. A. Jakobsen, *Comput. Chem. Eng.* 30, 535 (**2006**).
16. C. A. Dorao and H. A. Jakobsen, *Chem. Eng. Sci.* 61, 7795 (**2006**).
17. R. B. Diemer and S. H. Ehrman, *Journal of Powder Technology* 61, 7795 (**2006**).
18. J. C. Barret and N. A. Webb, *J. Aerosol Sci.* 29, 31 (**1998**).
19. A. T. Suddha and T. M. Mark, *Aerosol Science* 35, 889 (**2004**).
20. A. G. Gerber and A. Mousavi, *Applied Mathematical Modelling* 31, 1518 (**2007**).
21. J. A. Schwarz, Dekker Encyclopedia of Nanoscience and Technology, 1st edn., Mercel Dekker. Inc, New York (**2004**).
22. K. F. Sheldon, Smoke Dust, and Haze: Fundamentals of Aerosol Dynamics, 2nd edn., Oxford, New York (**2000**).
23. K. Ashish and D. C. Panagiotis, *Chem. Engng. Sci.* 54, 2669 (**1999**).
24. S. E. Pratsinis, *J. Collide. Interface Sci.* 124, 416 (**1988**).
25. E. L. Sergey, Engineering and Scientific Computation Using Matlab, Rochester Institute of Technology, Wiley Interscience, New Jersey (**2003**).